GLOBAL JOURNAL OF PURE AND APPLIED SCIENCES VOL. 13, NO. 2, 2007: 285 - 294

 1SSN 1118-0579

MATHEMATICAL REPRESENTATION OF SEASONAL CYCLES OF AEROSOL OPTICAL DEPTHS AT ILORIN NIGERIA USING AERONET DATA

O. K. NWOFOR AND T. C. CHINEKE

(Received 2 June 2006; Revision Accepted 15 September 2006)

ABSTRACT

In this work, Aerosol Optical Depth (AOD) data for six years (1998-2003) based on the National Aeronautics and Space Administration (NASA) Aerosol Robotic Network (AERONET) measurements for Ilorin, Nigeria (8^0 32'N; 4^0 34'E) are analyzed to study the seasonal pattern. The analyses show that there is a distinct seasonal cycle of AOD in Ilorin with peaks in the dry season and troughs in the wet season. Mathematical expressions are fitted to the observed periodic cycle using a model of the form $Y(t) = P_1 + P_2 \sin\left[\frac{\pi(x - P_3)}{P_4}\right]$ where Y(t) =AOD at time t, and P_1, P_2, P_3 and P_4 are parameters representing the annual average, seasonal modulation amplitude, phase and period respectively. The parameters are deduced iteratively based on the least square best fits to the 1998/1999 AOD time series which have the most data density of the 6 years series studied. The model reveals seasonal modulation amplitude for the peak solar wavelength (AOD_{500nm}) of ~0.327 over an annual mean value of 0.513. In order to minimize errors with models that estimate aerosol radiative and climatic effects at the site and other West African locations it is recommended that the seasonal AOD averages be used instead of the annual averages. The present results are useful for filling the gaps in AERONET time series, which are common due to instrument failure and for predicting AOD trends at the site.

KEY WORDS: Aerosols, Aerosol Optical Depth, Seasonality, AERONET, and Ilorin

1.0 INTRODUCTION

Aerosol Optical Depth (AOD) is, and will probably continue to be, the most difficult input parameter to obtain for models that estimate solar radiation at the earth's surface. This is due to large spatial and temporal variability. The AOD varies with the amount of aerosols of different sizes and number concentration, their chemical composition and the wavelength of the incident radiation (Bergin, 2000). Hence variations in aerosol source outputs, and possible transformations in aerosol size and chemical properties amongst other changes result in variations in AOD. These variations can be at varying temporal scales such as diurnal, seasonal, annual and long-term scales as well as on spatial scales spanning local to regional and global.

The seasonal behavior of AOD is brought about by processes associated with the production, transformation and removal of aerosols in the atmosphere (Heintzenberg, 1994), if such processes show seasonal character. Evaluation of seasonal character is useful for proper quantification of aerosol radiative effects on a regional scale (Markowicz et al, 2003) as well as for projecting these to the long term, which can help in predicting the AOD when data is not available as well as for modeling the associated influences of AOD variability in a region. A study of seasonality in AOD is a significant step in extracting aerosol life-cycle dynamics in a region, and for discussing the associated implications on weather and climate.

Several analyses of AOD variability show pronounced seasonal variations indicative of the variations in source strength and the effects of the weather. The sensitivity of aerosols to particular weather factors is peculiar to the location of a site. Weather parameters like wind for instance tend to influence the growth of aerosol particles in marine environments. (Smirnov et al, 1996; Smirnov et al, 2003). Rising Relative Humidity (RH) could tend to have similar growth effects because of the hygroscopic nature of marine aerosols (Heintzenberg, 1994). At sites that are not far from the aerosol sources, transport may be less influential so that weather parameters such as temperature and rainfall tend to take precedence over wind and humidity in determining aerosol variability. At some locations, especially in the polar climates (Ruuskanen et al, 2003) as well as temperate climates (Cheymol and De Backler, 2004), seasonality of AOD is largely attributed to anthropogenic factors. In West Africa, seasonal aerosol sources arise mainly from the yearly harmattan dust and pre – farming season biomass burning with seasonality in growth and sink processes influenced mainly by temperature variations and inception, duration and magnitude of rainfall.

Long-term projections of seasonal AOD are achieved through analysis of growth in the AOD time series over a long period. Inter annual and long-term trends in AOD for West African sites are mostly constrained by short time series (less than 10 years). This situation seems to improve with the inception of the AERONET database.

In this work data Aerosol Optical Depth over Ilorin, Nigeria for a six-year period (1998, 1999, 2000, 2001, 2002 and 2003) is used to asses the seasonal cycle. Mathematical expressions are used to fit the observed cycles with the aim of using them to predict the yearly variations. This will be useful for filling the gaps, which are common with AERONET measurements, and for projecting the measurements to the long term.

2.0 DATA AND SITE DESCRIPTION

The data were obtained from the Aerosol Robotic Network (AERONET) database. The AERONET network consists of a ground based remote sensing programme that was established to assess aerosol optical properties and validate satellite data (Holben, et al, 1998). The network is operated by the National Aeronautics and Space Agency-Goddard Space Flight Center (NASA-GSFC) and includes about 100 identical globally distributed sun- photometers. (AERONET site measurements at Ilorin, in West Africa have

O. K. Nwofor, Atmospheric Physics Group, Department of Physics, Imo State University Owerri, PMB 2000, Nigeria.
T. C. Chineke, Atmospheric Physics Group, Department of Physics, Imo State University Owerri, PMB 2000, Nigeria.

been made since 1998.) The sun-photometer data at the site are for 7 wavelengths, spanning through ultraviolet (UV), visible and Infra-Red (IR) wavelengths. These are 0.34μm, 0.38μm, 0.44μm, 0.5μm, 0.67μm, 0.87μm, and 1.02μm. The AOD data used are the so-called "level 2.0", which are cloud screened. The necessary algorithms for deriving AOD from sun-photometer data measurements are described by Dubovik and King, (2000) and Dubovik et al (2000).

The AERONET sensors are situated in a platform at the science building of the University of Ilorin, at height of 375m above sea level. The station is located at latitude $8^0$32N and longitude $4^0$34E (Figure 1).

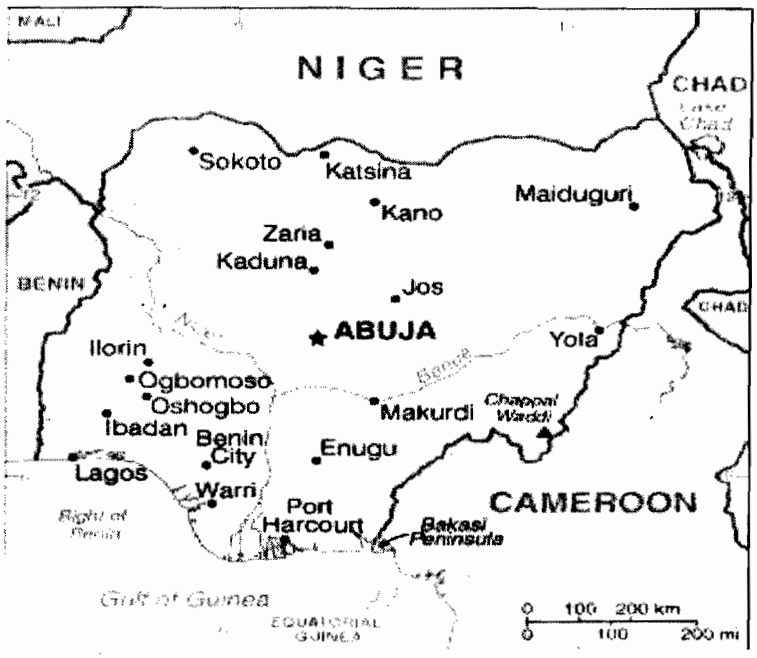

Figure 1: A map of Nigeria showing Ilorin, the study site

The climatic situation at Ilorin is well described by Udo (2004). Typical variations in weather parameters namely temperature, rainfall, relative humidity and wind speed, which were obtained from the Meteorological Department of the Federal Ministry of Aviation, are shown in figures 2, 3 and 4.

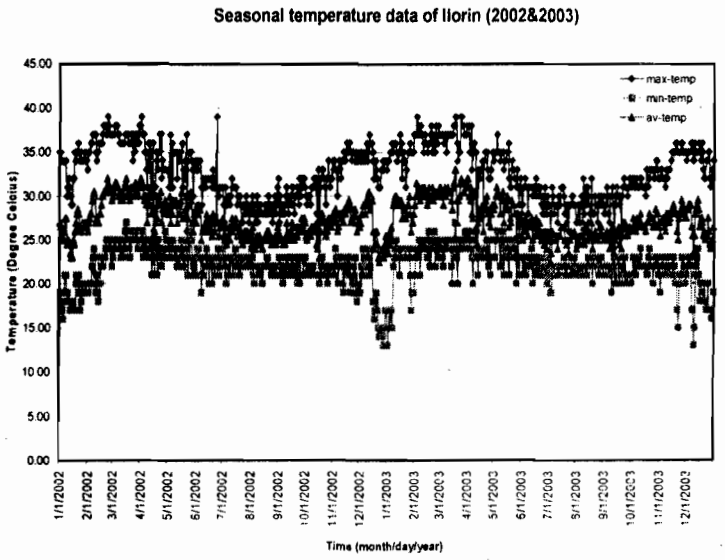

Figure 2: Typical seasonal temperature data for Ilorin. Period of measurement are in month/day/year, i.e. (mm/dd/yy). The **dry season months are from October to March of the succeeding year (month numbers – 11, 12, 1,** 2, 3), while the wet **season months are from April to September (month numbers – 4, 5, 6, 7, 8, 9)**

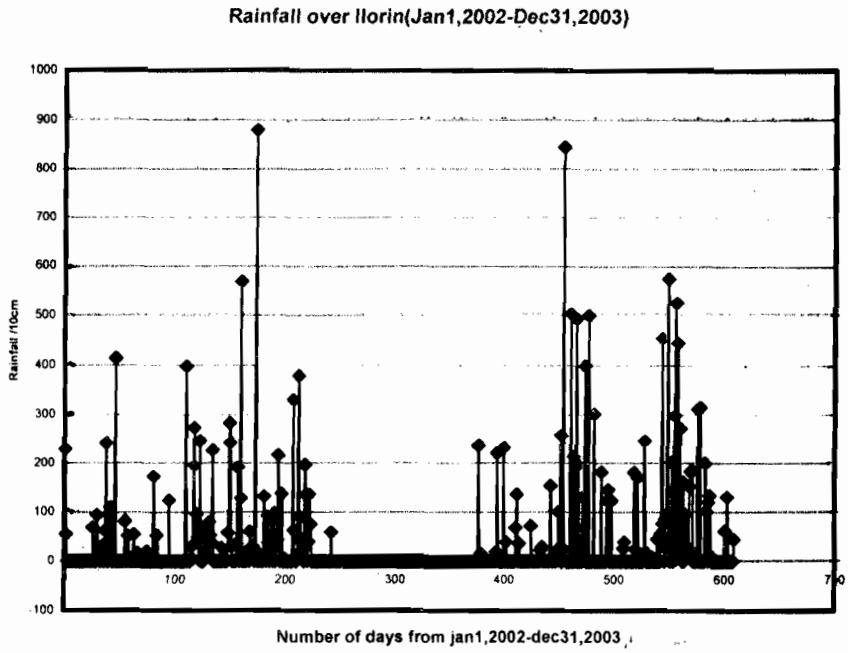

Figure 3: Rainfall pattern over Ilorin (January 2002, December 2003

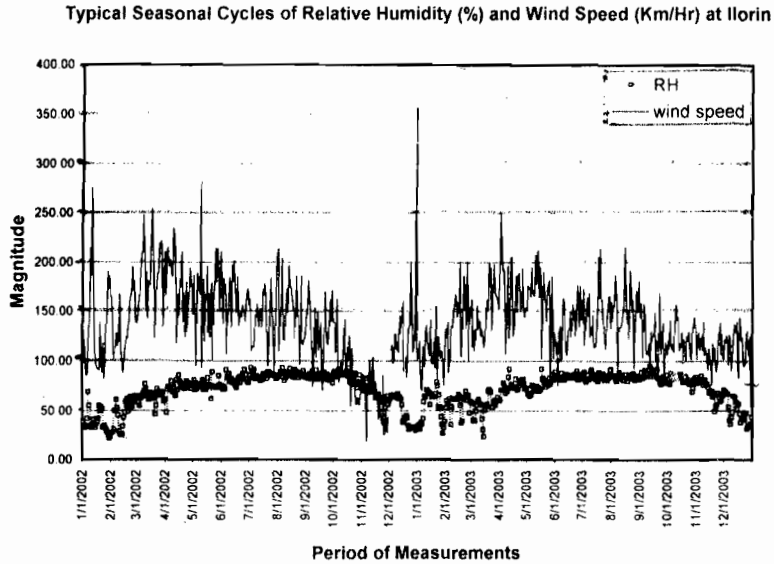

Figure 4: Seasonal cycles of relative humidity (%) and wind speed (km/hr) are Ilorin. Periods of measurements are in month/day/year i.e. (mm/dd/yy)

There are two seasons; the wet season and the dry season, brought about by the South Westerly (SW) and the North Easterly (NE) trade winds respectively. The SW blows from the Atlantic in the south ushering in rain to West Africa between the months of April to October, with annual rainfall in the range between 2000-2500mm and average seasonal temperatures between 26^0C – 28^0C. Between the ends of September to November, the North Easterly (NE) trade winds bring the dry season characterized by clear skies, moderate temperatures and low humidity in the area. A much drier period begins from the months of November to March of the succeeding year. This period witnesses a more vigorous NE, a very dry wind from the Sahara desert through the semi-arid north which brings the dusty harmattan period, characterized by heavy turbidity around December through March of the succeeding year. Although average wind speeds at the site could be about 150km/hr (figure 4), wind speeds during the harmattarn period may be as high as 200-250km/hr. . Ithough

average temperatures are ~ 27°C – 28°C, the dry season values are higher than the wet season values by about 5°C (Figure 2). Relative Humidity (RH) may fall as low as 25% in the dry season but remains above 80% for most parts of the wet season (Figure 4).

3.0 THEORETICAL CONSIDERATIONS

Our interest in this work is to describe the seasonal evolution of AOD variations at Ilorin Nigeria in fairly quantitative terms. A seasonal time series is characterized by its periodicity. Periodicity implies that similarities in the series occur after T basic time intervals where T is the period. Although the form of a time series model that would describe a given periodic behavior most appropriately is not usually obvious, two major considerations often motivate the choice of a particular model; First the model must be that whose characteristics reflect what is known about the function being modeled and second, the model must reproduce as closely as possible aspects of the series that are of uppermost importance to the modeler.

Generally, a periodic phenomenon in nature can be modeled by a sinusoid and its higher harmonics based on the Fourier Theorem (Edward and Hamson, 1996; Riley et al, 1998). Given a periodic series as function of x i.e. Y (x) with x having values 0, h, 2h, 3h... Nh (h=hours), with N odd, and the corresponding Y values are $Y_0, Y_1, Y_2 \ldots Y_N$, with $Y_N+1 = Y_0$, then the series can be fitted with a model that passes through all data points using a discrete Fourier series as follows;

$$Y(x) = \frac{p_0}{2} + \sum_{k=1}^{M}\left[p_k \cos\left(\frac{\pi kx}{L}\right) + q_k \sin\left(\frac{\pi kx}{L}\right)\right] + \frac{p_{M+1}}{2}\cos\left[\frac{(M+1)\pi x}{L}\right] \quad (1)$$

Where the first term of equation 1 is the average value of the Fourier coefficients, defined by

$$p_k = \frac{h}{L}\sum_{i=0}^{2M+1} y_i \cos\left(\frac{\pi kx_i}{L}\right) \qquad k= 0, 1, \ldots\ldots M+1 \quad (2)$$

$$q_k = \frac{h}{L}\sum_{i=0}^{2M+1} y_i \cos\left(\frac{\pi kx_i}{L}\right) \qquad k = 1, 2, \ldots\ldots M \quad (3)$$

And the period = 2L=(N+1) h and N=2M+1. A simpler model (not passing through all the data points) can be obtained by taking only the terms with the largest coefficients.

A much less simple model would be a "pure sinusoid" i.e. that involving only a single harmonic term, which could be of the form,

$$Y(x) = p_0 + p_1 \sin\left(\frac{\pi x}{L}\right) \quad (4)$$

Where p_0 is the average value and p_1 is the amplitude. Equation 4 is an appropriate model for a time series that exhibits considerable scatter especially if the interest is to model the periodic behavior of the mean value. It is well supported in the literature for describing several climatological parameters that undergo seasonal changes such as trace gas concentrations (Schneider, 2002; Zhao et al 2002). A modified relationship, which includes the phase constant, is used in this study.

4.0 METHODS AND RESULTS

4.1 Seasonal Patterns and Spectral Response

In our analysis of the AOD time series for the Ilorin site, we first show that the parameter follows an obvious seasonal pattern using Figure 5.

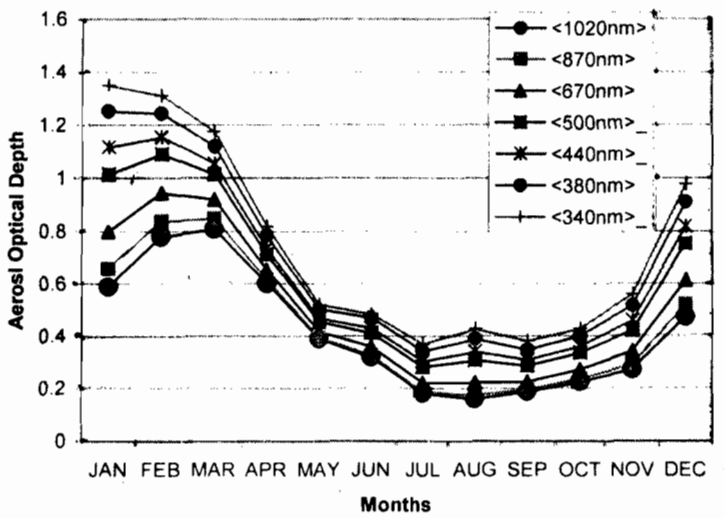

Figure 5: Multi-spectral seasonal patterns of AOD at the site based on means of monthly averages for the period 1998 – 2003 (The wavelengths are shown in the legend)

This is a plot of the average monthly values of AODs for the years 1998-2003. The monthly averages were computed as follows:

$$\tau_{month}=\sum\tau_{day}/N \quad (5)$$

Where τ_{month} is the monthly average of AOD, τ_{day} is the daily average and N is the number of days in a given month. The figure shows a smooth annual wave with a very defined crest between the months of January and March and a trough between July and August for the different wavelengths. The variations of the crests and trough are significant. The crest as the highest point of a periodic signal gives the peak position- in this case the month for maximum AOD variation. Similarly the trough signifies the month for lowest AOD variation. Figure 5 shows that the amplitudes of the crests and corresponding troughs vary for different wavelengths. This is because AOD depends on the wavelength. It is higher for the short solar wavelengths compared to wavelengths near the infrared end of the solar spectrum. The figure also shows that the months for maximum or minimum AOD within the year vary for different wavelengths. This is because particle sizes may vary at different months due to changing weather parameters, which tend to moderate size such as rainfall and wind speed. These observations are in conformity with the Mie theory, which requires that smaller particles scatter more efficiently than larger particles and more at shorter wavelengths (Bergin, 2000). The AOD curve shows greater sensitivity to wavelength in the dry season than in the wet season as shown in figure 5 due to the fact that a larger particle size spectrum is encountered in the dry season as compared to the wet season (Nwofor, 2006).

4.2 Model Fitting

A two-year multi-spectral daily averages data between the 25th of April 1998 and the 31st of December 1999 have been used to fit mathematical expressions for the seasonal patterns. The 1998-1999 (biennial) time series of AOD for the site was chosen because data was available for most of the days within the period totaling 489 measurements, compared to the other more sparse biennial series (2000-2001 periods with 294 measurements and 2002-2003 with 157 measurements).

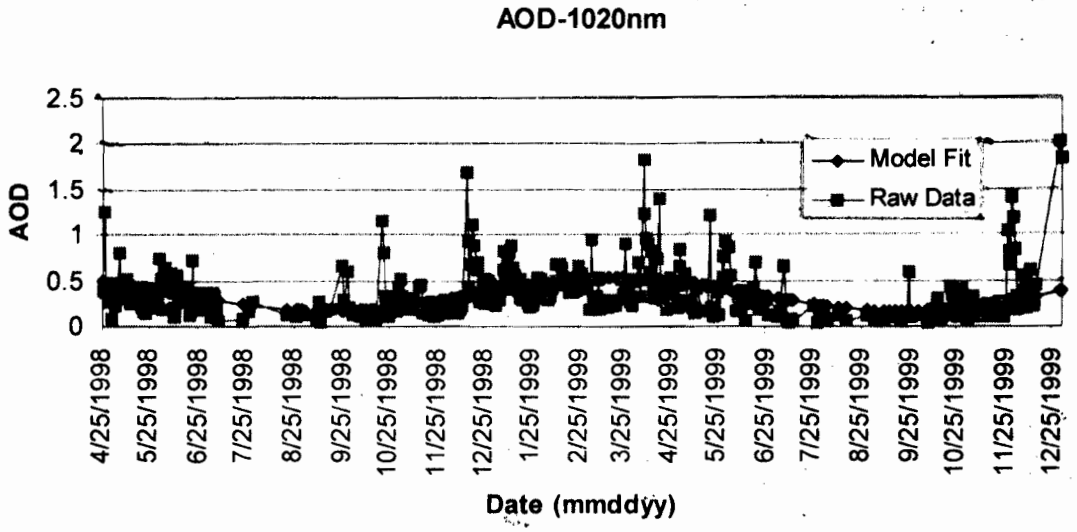

6a

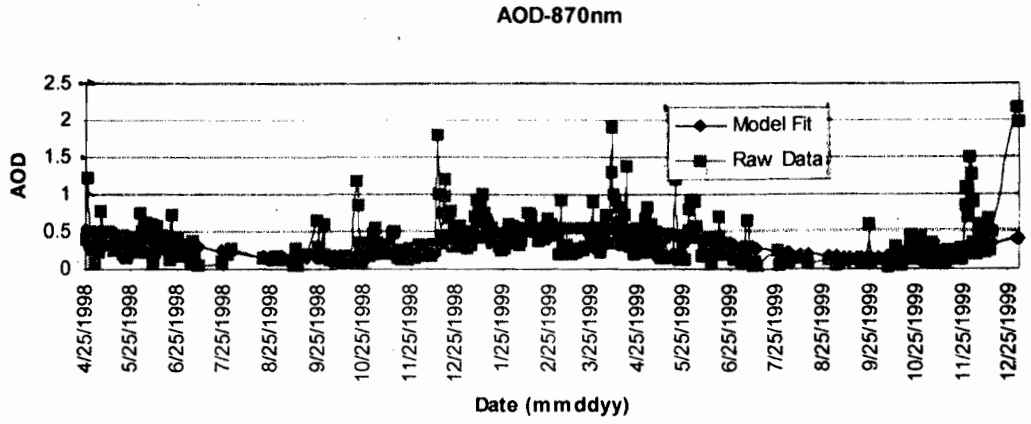

6b

AOD-670nm

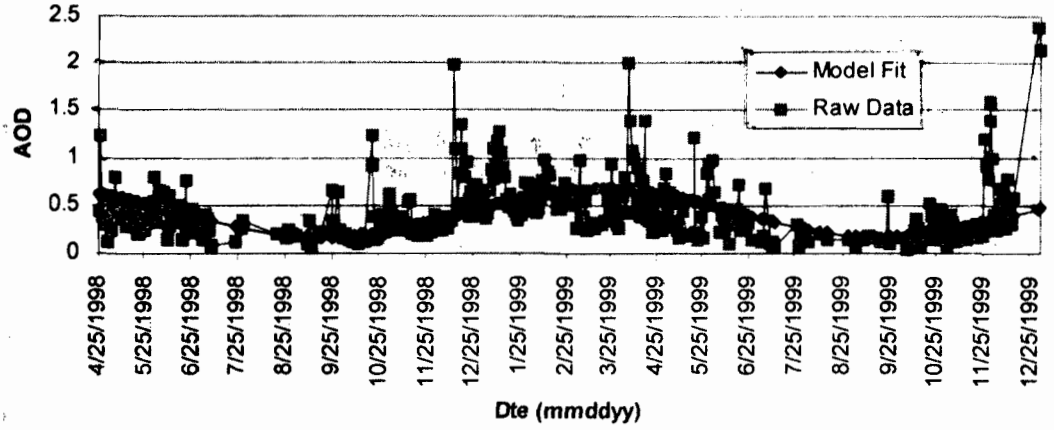

6c

AOD-500nm

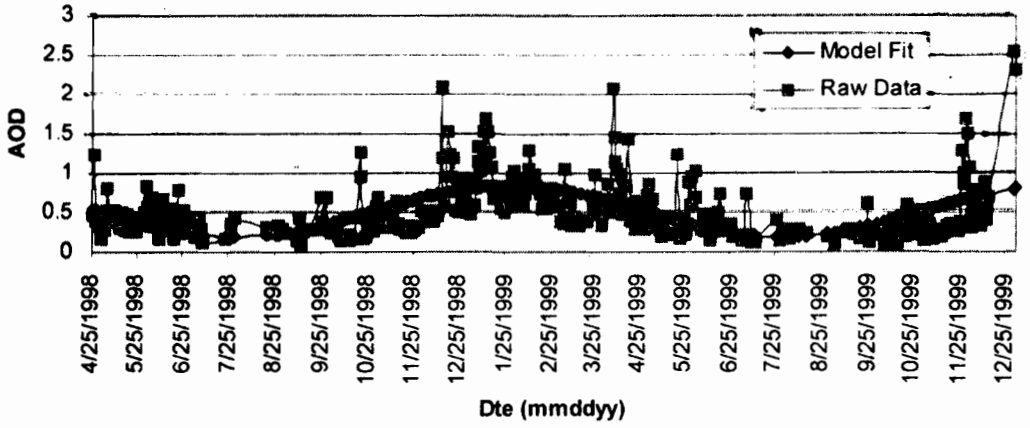

6d

AOD-440nm

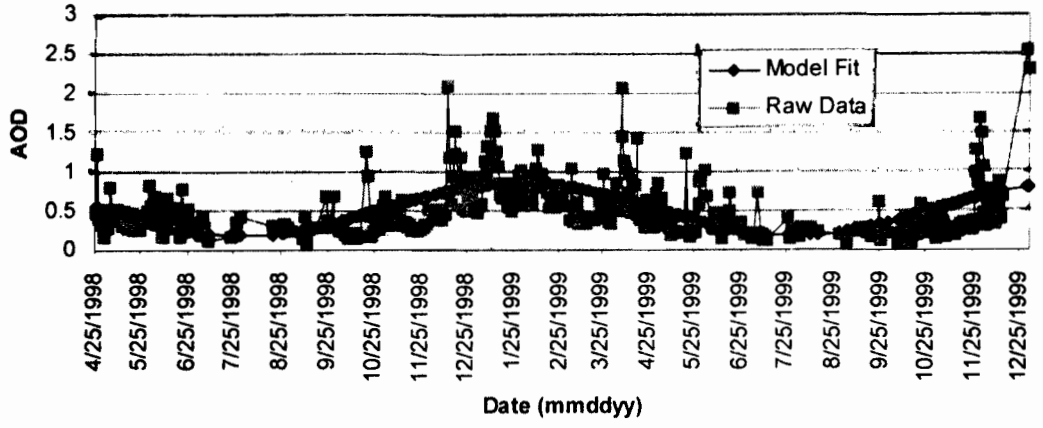

6e

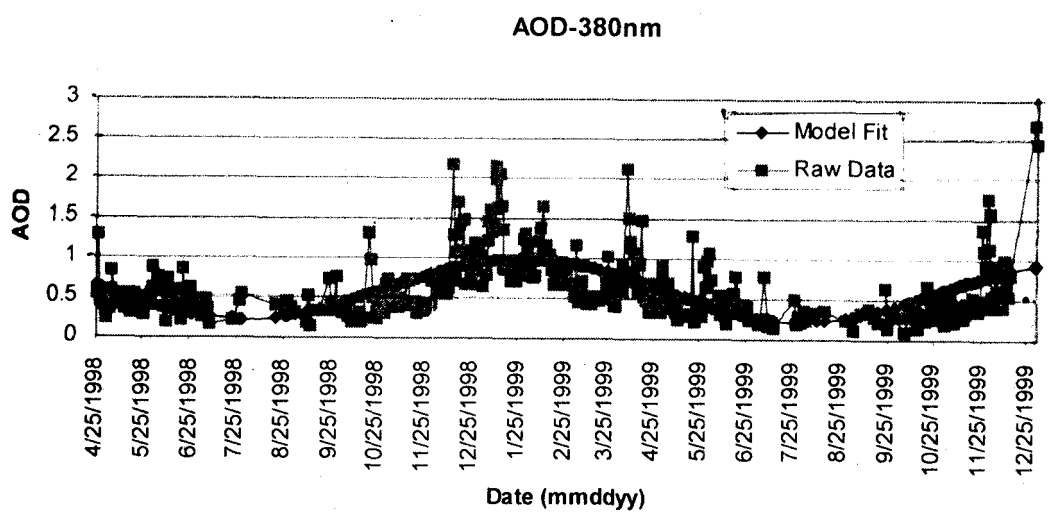

6f

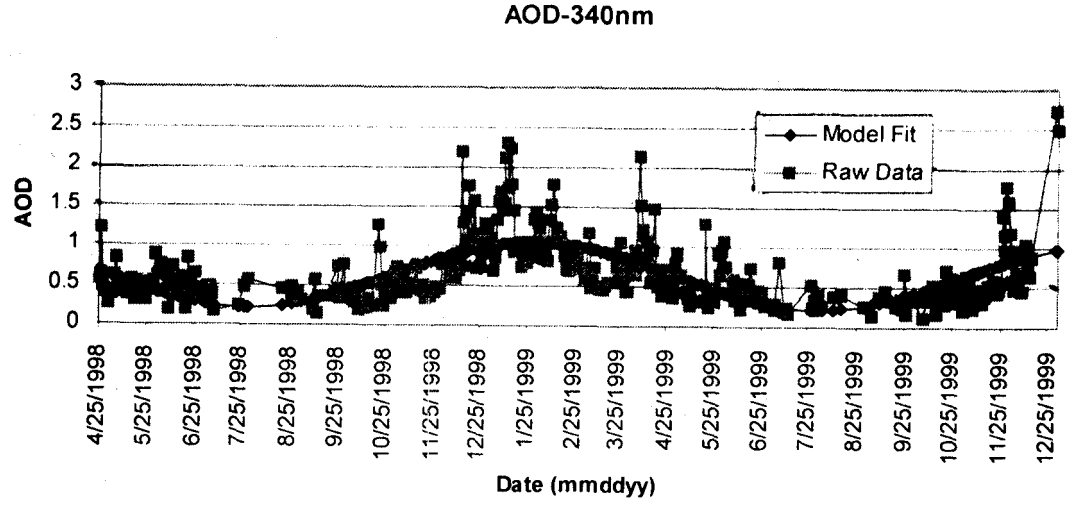

6g

Figure 6: Time series of AOD over Ilorin (1998/1999), with a sine curves fitted for the separate wavelength (a) 1020nm (b) 870nm (c) 670nm (d) 500mm (e) 440nm (f) 380nm (g) 340nm as indicated. The parameters of the sine fits are shown in table 2.

In figure 6(a-g) the AOD variations for the wavelengths 1020nm, 870nm, 670nm, 500nm, 440nm, 380nm, and 340nm respectively are shown for these series. The figures reveal strong seasonal cycles with period of a year (~365days). Since the variations are clearly periodic and can adequately be modeled using sinusoids, sine curves (shown in thick lines) were fitted to the data points using relations of the form i.e.

$$Y = P_1 + P_2 \sin\left[\frac{\pi(x - P_3)}{P_4}\right] \qquad (6)$$

The model represents the background levels of the AOD variations (Y) for each wavelength; where the parameters P_1, P_2, P_3 and P_4 are derived by iteration based on least square best fits to the data. They represent the annual average, amplitude of the seasonal modulation, the phase and the period respectively (note that the period $=2P_4$), while x represents time elapsed in days. The annual means deduced using the fits are in close agreement with those calculated from the raw data which shows that the iteration was good (Table 1).

Table 1: Comparison of arithmetic means of AOD for the bi-annual series (1998-1999) with means derived from the fitted seasonal trends

Wavelength	AOD Arithmetic means	AOD derived Trend fits	means from
1020	0.356	0.345	
870	0.377	0.359	
670	0.434	0.417	
500	0.519	0.513	
440	0.558	0.523	
380	0.622	0.606	
340	0.656	0.631	

Table 2: Parameters of the seasonal trend fits of the 1998/99 AOD Time series

Wavelength (nm)	Annual mean	Seasonal modulation amplitude	Phase	Chi-square
1020	0.345	0.178	-129.70	0.069
870	0.359	0.200	-129.25	0.076
670	0.417	0.250	-129.26	0.084
500	0.513	0.327	-132.43	0.093
440	0.523	0.342	-131.56	0.097
380	0.606	0.382	-131.56	0.105
340	0.631	0.410	-131.55	0.108

The parameters of the sine fits and the corresponding chi-square values (which indicate reasonable fits) are summarized in Table 2. The annual averages range from 0.345 (1020nm) to 0.631 (340nm). At the peak solar wavelength (500nm), the annual peak is 0.51 with seasonal modulation amplitude of 0.327. In all cases, the seasonal modulation amplitudes are more than 50% of the annual means. This means that significant errors would arise if annual means were used to model aerosol optical effects at the site at the peak of the seasons instead of the seasonal means.

The phase disparities of the sine fits for different wavelengths as can be seen in Table 2 are due to the fact that the inception of the annual peaks and lows are different for the various wavelengths as indicated in figure 5-whereas, for example, the 340nm and 380nm peaks occur in January, i.e. AOD equals 1.35 and 1.25 respectively, the 440nm, 500nm, and 670nm peaks are found to occur in February with Aerosol Optical Depths (AODs) of 1.16, 1.09, 0.95 respectively, while the 870nm and 1020nm peaks occur in March with AODs 0.85 and 0.81. The annual lows occur in July for the 340nm, 380nm, 440nm, 500nm and 670nm wavelengths –with associated AODs as 0.37, 0.34, 0.31, 0.28, and 0.18, respectively while the 870nm and 1020nm lows both with AOD 0.18 occur in August (Table 3).

Table 3: Months of annual peaks and lows of AOD showing differences at various wavelengths

Wavelenght (nm)	Peak month	AOD value	low month	AOD value
340	January	1.351	July	0.371
380	January	1.254	July	0.342
440	February	1.155	July	0.305
500	February	1.092	July	0.283
670	February	0.947	July	0.221
870	March	0.847	August	0.175
1020	March	0.808	August	0.175

5.0 DISCUSSIONS AND CONCLUSIONS

The observations regarding seasonal and spectral response of AOD at the Ilorin site are responses of aerosol sources to weather patterns in the area. First, the annual peaks in the months of January through March are in conformity with the seasonal weather scenario in the region. This is the dry season period, which is characterized by near zero precipitation, large temperature extremes and increased dust levels, which increase turbidities. The absence of rainfall (which is a major aerosol sink) enhances greater aerosol number concentration, which increases the AOD. Temperatures on the other hand favor photochemical reactions (Perrone et al. 2005), which lead to multiplicity in aerosol types and size, hence the observed increase in spectral sensitivity (indicative of multiple size scenario) compared to the wet period. Increasing wind speeds during the harmattarn period also increase size heterogeneity as these help to transport Sahara dust particles to the site which are superimposed on locally raised dust (Utah, 1995). Wet-season AOD on the other hand is lower mainly because of the absence of harmattarn dust and the fact that particles are easily removed by rain which peaks during this period. (Figure5). A look at figures 5 and 6(a-g) shows a more uniform variability in the background optical depth during the wet season compared to the dry season. This is because there is more homogeneity in the contributing particles because of the absence of the harmattan dust. The composition is typically of a single particle mode of fine dust, which is essentially raised

locally. This scenario results to a general reduction of AOD for the wet period compared to the dry period.

Given the large disparity between the seasonal AOD background values with the annual averages the use of annual averages to estimate AOD at this site would give rise to enormous discrepancies especially during the seasonal peaks. This is evident from table 4.

Table 4: Seasonal and annual statistics of Aerosol Optical Depths

Wavelength (nm)	Data	Mean	SD	SE
340	Overall	0.82757	0.56079	0.01935
	Dry	1.13018	0.58099	0.02812
	Wet	0.51358	0.31312	0.01543
380	overall	0.77836	0.54225	0.01871
	dry	1.06162	0.56736	0.02742
	wet	0.48409	0.31312	0.01543
440	Overall	0.71219	0.52103	0.01798
	dry	0.97064	0.55520	0.02684
	wet	0.44370	0.30349	0.01495
500	Overall	0.66953	0.50533	0.01744
	dry	0.90710	0.54629	0.02641
	wet	0.42273	0.30232	0.01489
670	Overall	0.57003	0.47242	0.01630
	dry	0.76684	0.52124	0.02519
	wet	0.36558	0.30183	0.01487
870	Overall	0.50420	0.44091	0.01521
	dry	0.66933	0.48960	0.02367
	wet	0.33266	0.29986	0.01477
1020	Overall	0.47428	0.41807	0.01442
	dry	0.61976	0.46321	0.02239
	wet	0.32314	0.29822	0.01469

The table shows the six years (1998-2003) overall means of the daily data together with their Standard Deviations (SD) and Standard Errors (SE). The dry season AOD range is between 1.13(340nm) to 0.62(1020nm), while the wet season range is from 0.51(340nm) to 0.32(1020nm). The annual overall average ranges from 0.77(340nm) to 0.47(1020nm). It can be deduced from the table that using annual averages instead of the seasonal means will under-estimate the dry-season OD and over-estimate the wet-season OD significantly.

This work shows that a clear seasonal cycle exists for aerosol optical depth variations at Ilorin, Nigeria, with peak values at the middle of the dry season and least values at the peak of the wet season. Equation 6 provides a reliable method of estimating the seasonal background levels of AOD at the site. It reliably defines the parameters such as the period, phase and seasonal modulation of AOD variations at each wavelength. The "annual average" (P_1) gives the average AOD level for defining the seasonal amplitude factor (P_2). Errors in the model can be reduced by using more data size to estimate the annual mean (P_1). Alternatively, the mode of the probability distribution of AODs could be used to provide even a more representative value of the annual average than the ordinary mean. In this work we have relied on the fact that the modeling of AOD is a practical process, which is based on data and/or assumptions on how the parameter to be modeled behaves under certain sets of conditions. In the present case, the data on AOD at Ilorin is provided by AERONET. Although a seasonal pattern might be apparent in the raw data (figures 6(a-g)), seasonality is only confirmed through an evaluation of the existing weather scenario at the site and the obvious AOD reactions to these. Consequently mathematical parameters are calculated and used to fit the appropriate seasonal function, using the region of the six-year time series with the most data density. With increased data length for such analysis deviations in the calculated annual averages are expected; also changes in weather patterns should produce shifts in the evaluated seasonal modulation factors and may impose changes in the annual averages. Hence the parameters in equations 1 and 2 provide base-line information but are essentially adjustable and their sensitivity to changing aerosol loading or weather patterns can be tested as more data become available. It is possible to project the observed seasonal cycles of Aerosol Optical Depths in the area to the long-term. The long –term trend can be estimated by adding a growth factor (linear, exponential e.t.c) to equation 2 which can then be written as

$$\tau(t) = \tau_0 + \tau_1 + \tau_2 \sin\left[\frac{\pi(t-\phi)}{6}\right] \qquad (7)$$

Where $\tau(t)$ is the AOD variation at time t, τ_0 is the annual mean AOD, τ_1 is the growth factor (deduced from the long-term trend) τ_2 is the seasonal amplitude modulation and t is the time in months.

ACKNOWLEDGEMENTS

The authors are grateful to Dr R.T Pinker, Principal Investigator of the Ilorin AERONET site for making available Aerosol Optical Depth data used for this work. Dr O.K Nwofor's research visit at the Institute for Meteorology and Climate Research, Forschungszentrum Karlsruhe, Germany in 2004. was useful in the preparation of this paper. Funding received from the German Academic Exchange Service (DAAD) for the visit is greatly appreciated.

REFERENCES

Bergin, M. H, 2000. Aerosol radiative properties and their impacts in ERCA Vol 4: From Weather Forecasting to Exploring the Solar System, edited by C.F Boutron. EDP. Les Ulis, France, pp 51 – 59.

Cheymol, A. and De Backer, H., 2004. Retrieval of aerosol optical depth in the UV – B region from Brewer ozone measurements from 1984 – 2002. Poster presentation, European Research Course on Atmospheres, Grenoble France, January 2004.

Dubovik, O and King, M. D., 2000. A flexible inversion algorithm for retrieval of aerosol optical properties from sun and sky radiance Measurements. J Geophys. Res, 105, 20, 696, 2000.

Dubovik, O, Smirnov, A, Holben, B, King, M. D, Kaufman, Y.J, Eck, T. F, and Slusker, I., 2000. Accuracy assessment of aerosol optical properties retrievals From AERONET sun and sky radiance measurements. Journ Geophys. Res, 105, 9791- 9806, 2000.

Edward, D. and Hamson, M. J., 1996. Mathematical Modeling Skills. London, Macmillan.

Heintzenberg, J, 1994. The life cycle of the Atmospheric Aerosol. In ERCA Vol I: Topics in Atmospheric and Interstellar Physics and Chemistry. edited by C.F Boutron. EDP, Les Ulis, France pp 251 – 270

Holben B.N and Co-workers, 1998. AERONET – A Federated Instrument Network and Data Archive for Aerosol Characteristics. Remote Sens. Environ. 66, 1–16. 1998.

Markowicz K.M, Flatau, P.J, Quinn, PK, Carrico, C.M, Flatau, M.K, Vogelmann, A. M, Bates, D, Liu, M, and Roth, M. J., 2003. m\. Influence of relative humidity on aerosol radiative forcing: An ACE-Asia experiment Perspective. Journ. Geophys. Res.108, No D23, 8662, doi; 1029/20025D003066, 2003

Nwofor, O. K., 2006. Seasonality of aerosol optical optical depth over Ilorin Nigeria. Unpublished PhD thesis, Department of Physics, Imo State University Owerri Nigeria.

Perrone, M.R, Santesse, M, Tafuro, A. M, Holben, B, and Smirnov, A, 2005. Aerosol load characterisation over south-east Italy for one year of AERONET sun-photometer measurements.Atmos.Res 75 Pp 111-133

Riley, K. F., Hobson, M. P. and Bence, S. J. 1998 Mathematical Methods of Physics and Engineering. London, Cambridge University Press 345

Ruuskanen T.M, Reissell A, Keronen P, Aalto P, Laakso L, Gronholm T, Hari P, and Kulmala M, 2003. Atmospheric trace gas and aerosol particle concentration measurements in Eastern Lapland, Finland 1992 – 2001. Boreal Environment Research 8: 335 – 349.

Schneider, M., 2002. Continuous Observations of Atmospheric Trace Gases by Ground-based FTIR Spectroscopy at Izana Tenerife Island. Unpublished PhD Thesis University of Karlsruhe Germany.

Smirnov, A, Onell, N. T, Royer, A. and Tarussor, A,, 1996. Aerosol Optical depth over Canada and the link with synoptic air mass types. Journ. Of Geophys. Research 101, (014): 19299 – 19318.

Smirnov, A, Holben, B. N, Eck, T. F, Dubovik, O, and Slutsker, I. 2003. Effect of wind speed on columnar aerosol optical properties at Midway Island. Journ. Geophys. Res. 108 (D24 4802): doi: 10.1029/2003/JD 003879

Udo, S. O., 2004. Characteristics of diurnal pattern of downward infrared radiation at Ilorin Nigeria. Nig Journal of Physi. 16 (1) : 126-130

Utah, E. U., 1995. Aerosol optical density during the Harmttan at Jos, Nigeria. Nig. Journ of phys. Vol.7.(1995)Pp 67 –71.